Intermolecular potential models for anisotropic molecules, with applications to N_2, CO_2, and benzene*

T. B. MacRury† and W. A. Steele

Department of Chemistry, Pennsylvania State University, University Park, Pennsylvania 16802

Bruce J. Berne

Department of Chemistry, Columbia University, New York, New York 10027
(Received 26 February 1975)

Three representations of the angle-dependent intermolecular interactions of nonspherical molecules are compared with one another and with experimental data for nitrogen, carbon dioxide and benzene. The models are the atomic, Kihara core, and overlap. The effect of including quadrupolar terms in the potential functions is also considered. It is found that the theoretical virial coefficients are not greatly altered when the quadrupole terms are added, at least at the temperatures corresponding to the experimental ranges for the molecules chosen. However, the theoretical solid state heat of sublimation and, to a lesser extent, the crystal lattice parameter, do change significantly. Satisfactory fits to the experimental second virial coefficients and the solid state data were obtained by varying ϵ, σ, the well-depth and range parameters, while fixing the other constants appearing in the models (such as the parameter specifying the nonsphericity) at reasonable values. Quantities of interest, including the equilibrium distance, angular configuration, and dissociation energy of the van der Waals' dimer, are estimated from the best-fit potential functions. It is concluded that all three models are approximately equivalent when the molecules are only slightly nonspherical and that there is sufficient flexibility in the models to give good fits to the data even for strongly nonspherical molecules. It appears that the representations of the N_2, CO_2, and benzene interactions derived here are sufficiently realistic to warrant their use in future work.

I. INTRODUCTION

As one progresses from spherical to nonspherical molecules, the difficulties involved in developing adequate models for the intermolecular interactions increase greatly, especially if one hopes to obtain a potential function capable of accounting for the properties of the solid and liquid phases as well as those of the imperfect gas. Even for a molecule as simple as nitrogen, one should include the electrostatic interactions (primarily quadrupolar in this case) as well as the effect of nonsphericity upon the repulsive overlap and attractive dispersion energies. Oddly enough, the majority of the theoretical studies dealing with properties that are dependent upon intermolecular interactions are based on models that include either the interactions of the permanent multipoles or the shape effects, but not both.[1]

An additional difficulty encountered in current treatments arises from the lack of a theory that would serve as a reliable guide to a unique model for the nonelectrostatic part of the interaction between nonspherical molecules. Consequently, a number of models are being explored by various workers, including the Kihara core model[2-3] (and a recent modification[4]) and the "atomic" model,[5-15] among others. Although both of these appear to be capable of giving reasonably accurate representations of selected molecules, they suffer from practical defects. In particular, let the intermolecular interaction energy of molecules 1 and 2 separated by a distance r and with Euler orientations angles Ω_1 and Ω_2 in coordinate axes defined relative to **r** be denoted by $u(r, \Omega_1, \Omega_2)$. The basic Kihara core model then consists in assuming that

$$u(r, \Omega_1, \Omega_2) = u(r/\rho) \quad , \tag{1.1}$$

where ρ is the shortest distance between two nonspherical "cores" with orientations Ω_1, Ω_2, and $u(r/\rho)$ is a suitable function such as the inverse 6–12 power law that is so often employed in modeling the interactions of spherical atoms. The difficulty in using the Kihara model occurs when one attempts to calculate ρ for given Ω_1, Ω_2; even though the theory is valid only for convex core shapes (a serious limitation in itself), the evaluation of the minimum distance between two such cores with arbitrary orientations is far from trivial. For example, the computer time would appear to be sufficient to prevent serious attempts at Monte Carlo or molecular dynamics studies of dense phases of these molecules. In addition, it is difficult to use this model to evaluate the librational force constants that characterize the torsional Raman and infrared frequencies observable either as lattice modes of the solid or in the dimeric "van der Waals molecules" present in low temperature gases.[16-19] If an interacting molecule is represented by n "atoms," these difficulties can be avoided. One writes

$$u(r, \Omega_1, \Omega_2) = \frac{1}{n^2} \sum_{i,j=1} u\left(\frac{r_{ij}}{\sigma}\right) \quad , \tag{1.2}$$

where r_{ij} is the distance between atom i in molecule 1 and j in molecule 2, and $u(r_{ij}/\sigma)$ is again taken to be a function of the Lennard-Jones type. (A single value of well depth and of σ implies that all atoms are identical—this constraint is clearly not crucial.) If the coordinates of atom i in the molecule are given by L_i, β_i, α_i, the distance r_{ij} can be obtained by a coordinate transformation from the molecule-fixed system to the **r**-fixed axes.[20] These operations present no particular difficulties for "diatomic" molecules, or even for triatomic, linear models. However, as the number of atoms per molecule increases and as the shape becomes more complex so that the molecule-fixed atomic posi-

tions are no longer on an axis of symmetry, the evaluation of the summation in Eq. (1.2) becomes prohibitively time consuming, especially when averages over all configuration space are required (as in calculations of the second virial coefficient or of liquid state properties).

Recently, another approach to the problem of dealing with nonspherical shapes was proposed[21] which does not suffer from the defects noted in the atomic and Kihara core theories. In this model, which is called the overlap model, two interacting spheroids of fixed center of mass position and fixed orientation are assumed to have a repulsive potential which is directly proportional to the intermolecular overlap volume. The mass distribution of each spheroid is assumed to be given by a spheroidal Gaussian distribution. The computed overlap volume is a function of the orientational angles and the relative distance between the center of mass. Its specific form is $\epsilon \exp(-r^2/\sigma^2)$, where ϵ and σ, the range and energy parameter depend on the relative orientations of the two spheroids. The specific form of ϵ and σ are assumed to reflect the symmetry of the molecules, and are then used in connection in a class of functional terms like $\epsilon\phi(r/\sigma)$. In the overlap model one characterizes shape by defining ϵ, σ, the well-depth and range parameters of the intermolecular potential, to be dependent upon orientation. Specifically, for two identical ellipsoids of revolution, one writes

$$\epsilon(\Omega_1, \Omega_2) = \epsilon(1 - \chi^2 \cos\Theta_{12})^{-1/2} \quad , \tag{1.3}$$

where Θ_{12} is the angle between the symmetry axes of the ellipsoids; and

$$\sigma(\Omega_1, \Omega_2) = \sigma\left(1 - \chi \frac{\cos^2\Theta_1 + \cos^2\Theta_2 - 2\chi\cos\Theta_1\cos\Theta_2\cos\Theta_{12}}{1 - \chi^2\cos^2\Theta_{12}}\right)^{-1/2} , \tag{1.4}$$

where Θ_1, Θ_2 are the polar angles between the molecular axes and $\mathbf{r}$, and χ is a shape parameter defined as

$$\chi = \frac{\kappa^2 - 1}{\kappa^2 + 1} \quad , \tag{1.5}$$

where κ is the ratio of the length of the principal axis of the ellipsoid to the length of the axis perpendicular to it. It is evident that the relationship between interaction energy and molecular orientation is explicit and reasonably simple in the overlap model; that no sums are involved; and that the formulation is flexible in the sense that any appropriate distance-dependent function can be utilized, from a hard-core model (with an angle-dependent σ) to an inverse power law with arbitrary indices. For example one might wish to vary the form of the potential in an extension[22,23] of the perturbation theories of dense fluids of spherical molecules. These theories[24] generally are based upon the idea that pair correlation functions at high densities are determined primarily by the repulsive part of the intermolecular potential. Thus, it is convenient to work with a model where the attractive energies can be omitted when appropriate without redoing the entire problem. (In fact, all three of the models discussed here share this desirable feature.)

In this paper, the linear Kihara core, the "diatomic" and the (prolate) overlap models are first compared for inverse (12,6) power laws and it is shown that the three theories are similar, especially if the parameter of the nonsphericity is varied to maximize the correspondence. Subsequently, data for three specific molecules are fitted to theory; the systems chosen for study include N_2, a short linear molecule with a relatively small quadrupole moment; CO_2, a long linear molecule with a relatively large quadrupole moment; and benzene, a planar molecule that also possesses a relatively large quadrupole moment.

It is conventional to test intermolecular potentials by comparison of theoretical and experimental second virial coefficients. However, it is well known that this procedure is insensitive to the functional dependence of the energy, and serves primarily to determine the two parameters ϵ, σ. Of course, the interactions of nonspherical molecules involve at least three (ϵ, σ and a shape parameter), even if values for the permanent electric moments are obtained from other sources. Indeed, we will see that the virial coefficient data for benzene are not even of sufficient quality to determine unambiguous values for two of these parameters. Consequently, other comparisons between experiment experiment and theory are needed. Of the various possibilities, we have chosen the crystal packing distances and heat of sublimation as most suitable, and have therefore chosen potential functions for N_2, CO_2, and benzene that are consistent with these data as well as the virial coefficients.

All three models can be fitted to the N_2 data using an inverse (12, 6) power law for the distance dependence of the potential together with the known quadrupole–quadrupole interaction. The (12, 6) diatomic and triatomic models plus quadrupolar terms can be fitted to the CO_2 data. However, the overlap model (plus quadrupolar term) is inadequate if either the (12, 6) or a (28, 7) function is used; it is surmised that a power law with indices intermediate between these two would be more successful. In the benzene case, the only model tested was the overlap, quadrupolar potential. (The application of the Kihara core model to the CO_2 and benzene data has been discussed previously[2,3]). It was found that the (12, 6) power law is inadequate, but the (28, 7) potential is reasonably successful in representing the benzene interactions. The best fit potentials are utilized to compute a number of relevant quantities such as angular correlations and the associated virial coefficient for depolarized light scattering, and the dissociation energy and stable molecular configurations in the van der Waals dimers of these molecules.

In attempting to compare the potential functions produced by these models which depend upon the four variables r, Θ_1, Θ_2, ϕ, several techniques may be employed. Two obvious choices are the following: fix the values assigned to all variables but one (plots of energy versus distance, for example) or two (contours of constant energy as a function of Θ_1 and Θ_2 at fixed r, ϕ); or the coefficients in an expansion in orthogonal functions can be evaluated.[25] Although these expansions are

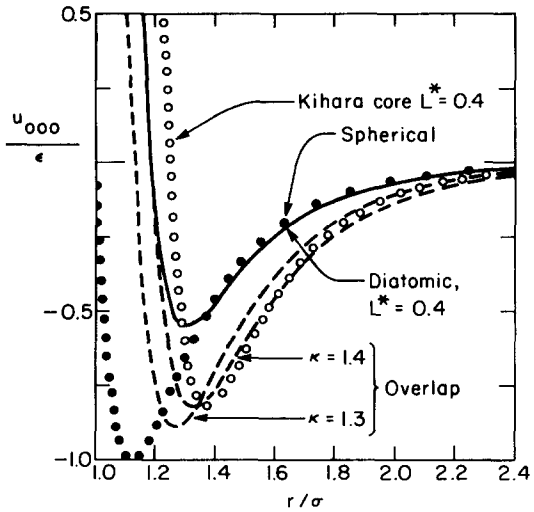

FIG. 1. The angle-averaged interaction energy is plotted versus reduced distance for three models of linear molecules. Since κ is the ratio of long to short axis length in the overlap model, it is comparable to $(\sigma+L)/\sigma=1+L^*$, where L^* is the separation between atomic centers in a diatomic molecule. The distance where the energy passes through zero in the Kihara model is σ for a parallel configuration and $\sigma+L$ for an end-to-end arrangement, so $1+L^*$ is the axial ratio in this case as well.

convergent in all cases if the variables chosen are the angles Θ_1, Θ_2, ϕ (giving r-dependent coefficients), the convergence can be quite slow for small r at large values of the nonsphericity parameter. (This is a consequence of the large changes in energy with orientation at small, fixed separation distances.) Thus, we will present curves of some coefficients in the angular expansion of the energy for those cases where the parameters of the nonsphericity can be chosen to be small, but will use the other methods of exhibiting the potential functions for CO_2 and benzene, which appear to be too far from spherical to allow one to use the orthogonal function expansion with a reasonable number of terms.

II. COMPARISON OF POTENTIALS FOR LINEAR MOLECULES

In this section, the expansion in orthogonal functions for the potential will be written:

$$u(r,\Theta_1,\Theta_2,\phi)=4\pi\sum u_{ll'm}(r)P_{lm}(\Theta_1)\times P_{l'-m}(\Theta_2)\exp(im\phi)\ , \qquad (2.1)$$

where the P_{lm} are associated Legendre polynomials. The leading term in this series $[u_{000}(r)]$ is the angle-averaged energy, and the higher terms give a measure of the angle dependence of this quantity. For symmetric linear molecules, only coefficients with even l, l' are nonzero.

Figure 1 shows u_{000}/ϵ computed for three models. In all three cases, the distance dependence of the energy was assumed to be

$$u(x)=\frac{n\epsilon}{m-n}\left(\frac{m}{n}\right)^{m/(m-n)}\left[\left(\frac{\sigma}{x}\right)^m-\left(\frac{\sigma}{x}\right)^n\right]\ , \qquad (2.2)$$

with m, $n=12,6$. For the diatomic model, $x=r_{ij}$, the intermolecular atomic separation and $L=$ the intramolecular atomic separation ($L^*=L/\sigma$); for the Kihara model, $x=\rho$, the core separation and $L=$ the core length; for the overlap model, $x=r$, the intermolecular separation, with $\epsilon(\Omega_1,\Omega_2)$ and $\sigma(\Omega_1,\Omega_2)$ given by Eqs. (1.3) and (1.4), respectively. For reference, the (12, 6) Lennard-Jones function for spherical molecules is also shown. It is immediately evident that the three nonspherical models are qualitatively similar, and that the angle-averaged potentials all exhibit shallower minima at greater r^* than the curve for spherical molecules. The results for the overlap and the Kihara core models are closest to one another, for comparable values of the parameters of nonsphericity. (Evidently, $1+L^*$ is a length-to-thickness ratio that should be comparable to κ.) The difference in well depths observed for the diatomic and the other two models can be at least partially eliminated by comparison with u_{000}/ϵ for the diatomic model with a smaller L^*; however, the minimum will then occur at a different value of r^*.

Figures 2 and 3 show two of the coefficients of the angle-dependent terms in the expansion of $u(r,\Omega_1,\Omega_2)$. Again, the three models are qualitatively similar, with the diatomic model exhibiting shallower wells than the Kihara core or the overlap models. However, the well-depth differences are magnified by the change in scale relative to that for Fig. 1, and are actually rather insignificant (differences of ~0.1 for u_{200}/ϵ and ~0.01 for u_{220}/ϵ, compared to ~0.3 for u_{000}/ϵ). If the molecules under consideration possess an appreciable quadrupole moment Q, one finds that the quadrupolar contributions to u_{220}, u_{221} and u_{222} overwhelm the shape-dependent parts at distances greater than those that correspond to the steeply rising parts of curves such as the ones shown in Fig. 3. One can write the quadrupolar energy E_{QQ} as[26]

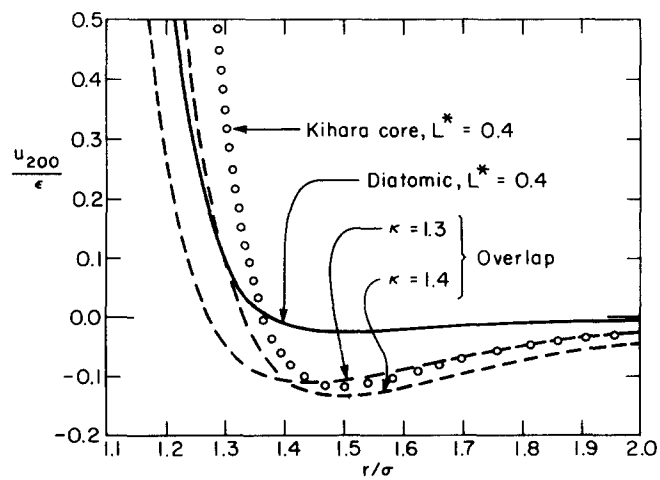

FIG. 2. The coefficient u_{200}, which is a measure of the angle dependence of the energy after averaging over orientations of one member of the pair, is plotted for the same models as in Fig. 1.

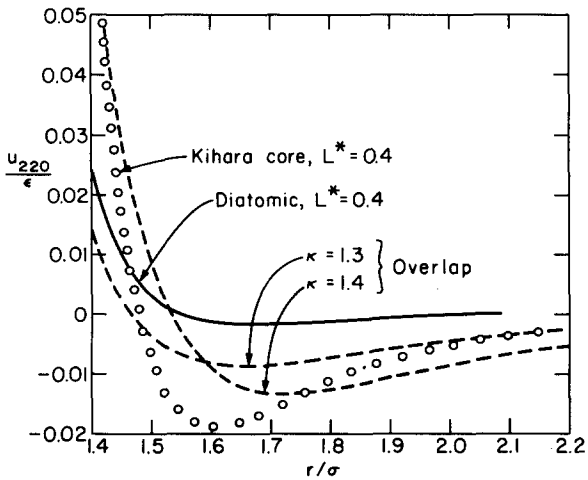

FIG. 3. The coefficient u_{220}, which is a measure of the angle-dependence of the energy after averaging over all values of the azimuthal angle ϕ, is plotted for the same models as in Figs. 1 and 2.

$$E_{QQ} = 4\pi [u_{220}^{(Q)}(r) P_{20}(\Theta_1) P_{20}(\Theta_2) + 2\, u_{221}^{(Q)}(r) P_{21}(\Theta_1) P_{2-1}(\Theta_2) \cos\phi + 2\, u_{222}^{(Q)}(r) P_{22}(\Theta_1) P_{2-2}(\Theta_2) \cos 2\phi] \; ; \qquad (2.3)$$

with

$$u_{220}^{(Q)}(r) = 6Q^2/r^5 \quad , \qquad u_{221}^{(Q)}(r) = 4Q^2/r^5 \quad , \qquad u_{222}^{(Q)}(r) = Q^2/r^5 \quad . \qquad (2.4)$$

This preliminary comparison indicates that the three models should give comparably good fits to experimental data, especially if one optimizes ϵ, σ, and the shape parameter. Of course, allowable molecular shapes are restricted to some degree by one's knowledge of bond lengths and van der Waals radii[27] and we have chosen to proceed by assuming reasonable values for L (or κ) and then optimizing ϵ and σ only.

III. NITROGEN

The second virial coefficients of nitrogen gas have been measured to good accuracy over a wide temperature range[28]; in addition, the heat of sublimation[29] and crystal structure[30] of the low temperature, low pressure phase of solid nitrogen are well known (cubic, α phase). All three potential models are capable of giving a good fit to these experimental data. The quadrupole moments[26,31] and shape parameters utilized are listed in Table I. In this case, the virial coefficients were fitted to theory for the diatomic and overlap potentials with and without including quadrupole interactions. The results listed in Table II show that the inclusion of these electrostatic terms hardly affects the virial coefficients; i.e., the angle averaging is quite effective in eliminating this contribution at the relatively high temperatures of the gas phase experiments. In contrast, the crystalline lattice contains molecules with fixed orientations; in calculating the theoretical ΔH_{sub} and lattice cell size a_0, the experimental values for these orientations were used to calculate the distance and value of the minimum intermolecular energy. One sees that the calculated quadrupolar energy amounts to roughly 10% of the total ΔH_{sub} for this crystal. Presumably, the results obtained using the Kihara core potential will be essentially the same; the values listed in Table II for this model were taken from an earlier study in which quadrupolar terms were omitted. Also listed are the parameters of the diatomic potential used by Schnepp *et al.*[10] in a successful calculation of the lattice frequencies of solid N_2, together with the "best" diatomic parameters deduced by Das Gupta *et al.*[22] primarily from a study of the liquid structure factor, but including results of other studies as well. It seems highly probable that all three models are capable of giving an adequate representation of the physical properties of nitrogen. The diatomic model has been used most extensively to date, although the quadrupole energy has not always been included in previous work. Of course, not all properties are sensitive to this term; in general, it should be most important in low temperature, high density phases where the orientational correlations are most pronounced. The importance of including a nonspherical shape is somewhat more difficult to assess. It is clear that the virial coefficients can be fitted using a spherical Lennard-Jones function, with and without quadrupole energies; Table II shows that the calculated ΔH_{sub} and a_0 for this potential agree with experiment if one includes the quadrupole terms. Presumably, the nonsphericity will play a more important role in developing adequate theories of the compressed liquid and solid. For example, it is hard to see how one can account for the $\alpha \rightarrow \gamma$ phase transition in the solid at high pressure if the only angle-dependent potential energies are quadrupolar, in view of the fact that the relative molecular orientations are quite different in the two phases.[30]

TABLE I. Selected experimental properties.

Molecule	Q (e.s.u. cm^2)	L^*	κ	ΔH_{sub} (kcal/mole)	a_0 (Å)
N_2	$1.5 \cdot 10^{-26}$ [a]	0.3	1.3	1.81[e]	4.00[f]
CO_2	$4.3 \cdot 10^{-26}$ [a]	0.8	1.8	6.4[d]	3.94[g]
C_6H_6	$5.6 \cdot 10^{-26}$ [b]	...	0.5	10.7[e]	7.29[h]

[a]See Refs. 26 and 31.
[b]See Ref. 39.
[c]See Ref. 29.
[d]See Refs. 12 and 32.
[e]See Ref. 37.
[f]See Ref. 30.
[g]See Ref. 33.
[h]See Ref. 36.

TABLE II. Calculated properties for nitrogen.

Model	ϵ/k (deg.)	σ (Å)	ΔH_{sub} (kcal/mole)	a_0 (Å)
Spherical (12,6), $\gamma=0$	94	3.70	1.51	4.04
Spherical (12,6), $\gamma=0.25$	94	3.70	1.84	4.00
Diatomic (12,6), $\gamma=0$	140	3.36	1.70	3.96
Diatomic (12,6), $\gamma=0.27$	139	3.34	2.04	3.88
Schnepp *et al.*[a] [diatomic, (12,6), $\gamma=0$]				
$L^*=0.33$	149	3.35	1.81	4.00
$L^*=0.25$	135	3.45	1.81	4.00
Overlap (12,6), $\gamma=0$	94	3.37	1.52	4.04
Overlap (12,6), $\gamma=0.40$	94	3.37	1.85	4.00
Kihara core (12,6), $\gamma=0$	119	3.13	...	...
Das Gupta *et al.*[b] [diatomic, (12,6) $\gamma=0$)]	140 ± 10	3.35 ± 0.05	...	...

[a]Reference 10. [b]Reference 22.

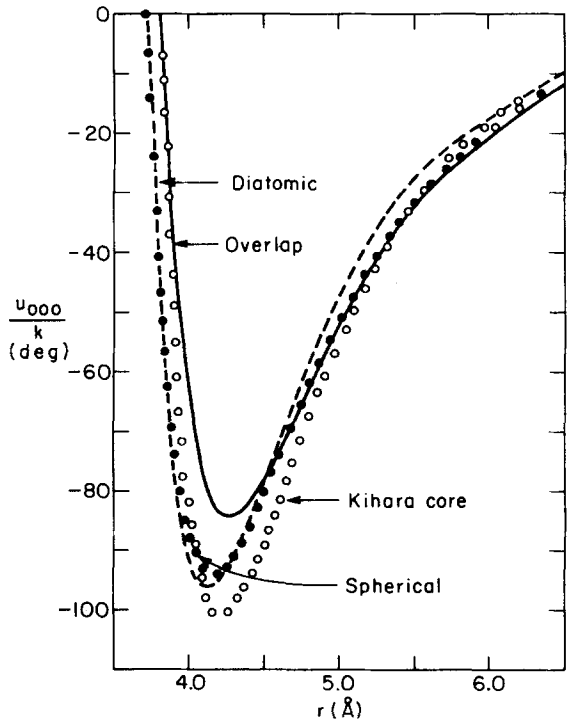

FIG. 4. The angle-averaged part of the interaction energy is shown here for four potential functions that reproduce the properties of nitrogen.

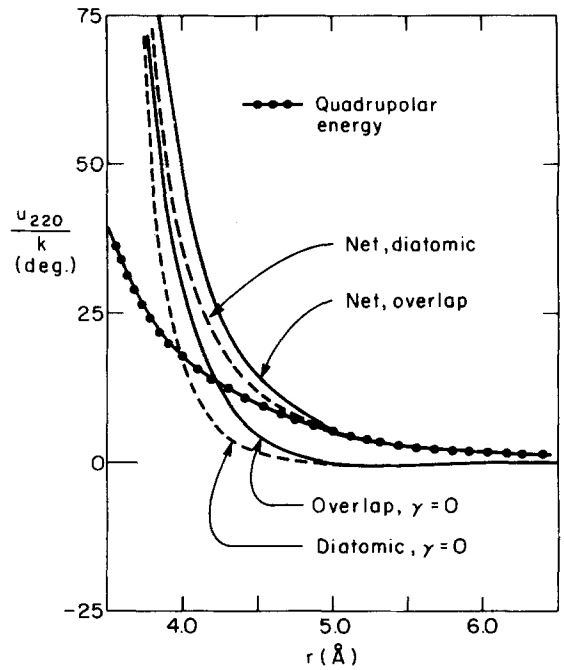

FIG. 6. The coefficient u_{220}, with and without the quadrupolar contribution, is shown for the models of Figs. 4 and 5.

We note that the potential parameters were derived in this work for N_2 by fitting theory to the experimental second virial coefficients. The inevitable uncertainties in the data give rise to a range of "best fit" ϵ and σ values, even for fixed L^*; simultaneous optimization of all three parameters would probably give perfect fits to the gaseous and solid data (i.e., within experimental error) in all cases.

Figures 4–7 show the components obtained for the spherical harmonic expansion of $u(r, \Omega_1, \Omega_2)$ for various models of N_2. Figures 6 and 7 illustrate the dominance of the quadrupolar terms in determining u_{220} and u_{221} at larger distance; Fig. 4 indicates that the fitting process gives rise to curves of the angle-averaged energy that do not differ greatly for the three models.

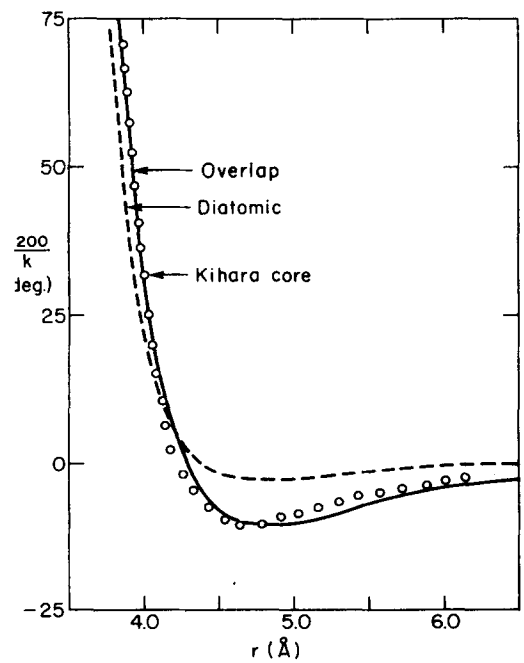

FIG. 5. The coefficient u_{200} in the spherical harmonic expansion of the interaction energy is shown for the same models of nitrogen as in Fig. 4 (Clearly, $u_{200} \equiv 0$ for the spherically symmetric potential.)

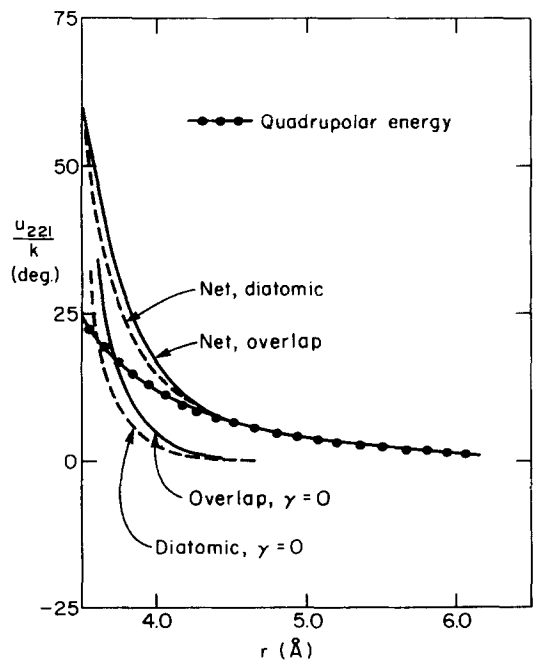

FIG. 7. The coefficient u_{221}, with and without the quadrupolar contribution, is shown for the models of Figs. 4 and 5.

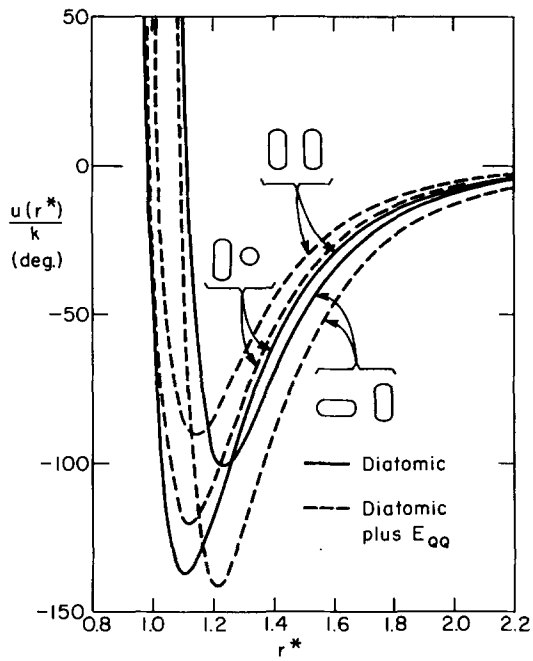

FIG. 8. The energy of interaction between two nitrogen molecules with fixed orientations is plotted as a function of the separation distance. The curves are for the best diatomic model, with and without quadrupolar energy E_{QQ}, and the orientations chosen are the following: parallel (θ_1, θ_2, $\phi = 90°$, 90°, 0°); T-shaped (0°, 90°, any value); and crossed (90°, 90°, 90°).

Of course, the spherical harmonic expansion is only one of several ways of presenting these potential functions; a second possibility is illustrated in Figs. 8 and 9, where curves of interaction energy are shown for pairs of N_2 molecules with fixed orientations. Figure 8 shows the potential versus distance for the diatomic model, with and without the quadrupolar term, and Fig. 9 shows the same curves for the overlap model. It is evident that the most stable $(N_2)_2$ molecule has the T shape, with a calculated dissociation energy and equilibrium separation distance of 282 cal/mole and 4.03 Å for the diatomic model (plus quadrupole) or 254 cal/mole and 4.29 Å for the overlap (plus quadrupole). These predictions are relevant to experimental studies of the van der Waals molecules which are currently under way.

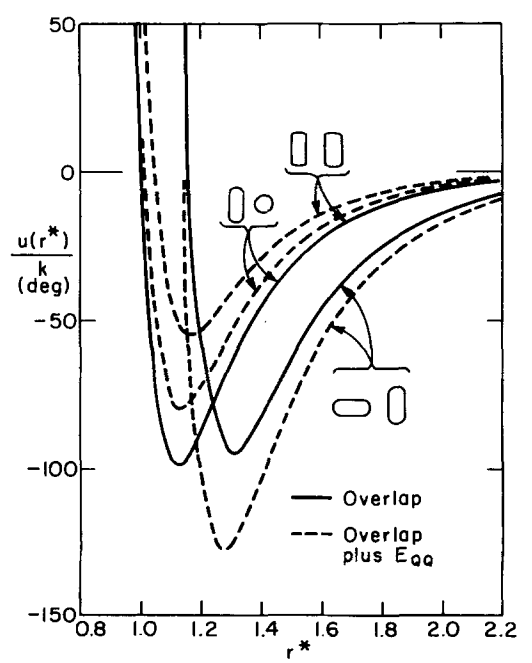

FIG. 9. The distance dependence of the interaction energy given by the overlap representation of nitrogen is shown for the same orientations as in Fig. 8, with and without quadrupole terms.

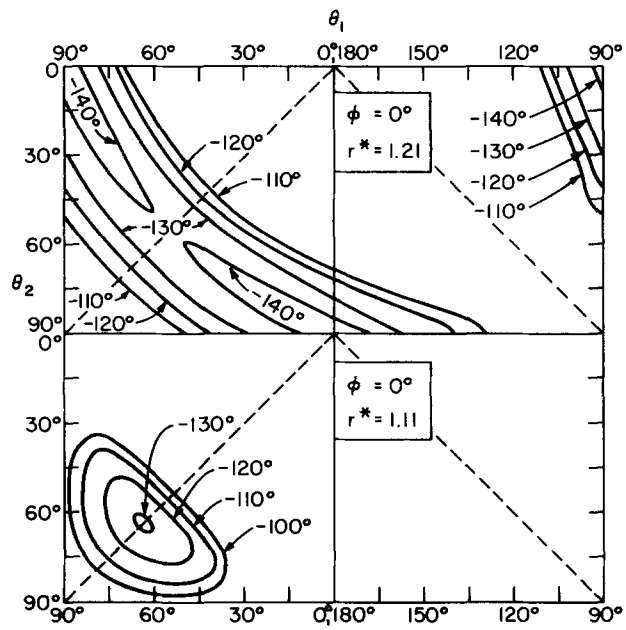

FIG. 10. Equipotential contours are shown for the diatomic model of interacting nitrogen molecules (including quadrupolar energy) for varying polar angles θ_1 and θ_2, but with ϕ and r^* fixed at the indicated values. The dashed lines indicate mirror planes of symmetry.

Yet another method of presenting the potential energies of the N_2–N_2 pairs is adopted in Fig. 10, which shows energy contour lines for variable polar angles Θ_1, Θ_2 with ϕ fixed to give a planar dimer, and at two different but fixed values of r^*. The curves shown are calculated for the diatomic model (plus quadrupole) at r^* corresponding first to the minimum in the energy for the T-shaped molecule and then for a somewhat smaller value of $r^* = 1.11$. (Although the X-shaped dimer has its minimum energy at this r^*, it is nonplanar and thus is not the configuration illustrated in the figure.) In fact, the most stable configuration of the planar dimer with $r^* = 1.11$ is with parallel axes but with both molecules canted at 63° to the intermolecular vector, rather than the 0° and 90° angles for $r^* = 1.21$ that is shown in the upper part of the figure.

The contour diagrams of Fig. 10 are useful in making theoretical estimates of the molecular orientations and librational frequencies in the solids. Although no quantitative conclusions can be drawn from the planar configurations of Fig. 10 ($\phi = 0°$), it is evident that the equilibrium orientations shift radically as r^* decreases and that the force constants for libration should increase rapidly as r^* decreases. Both predictions are

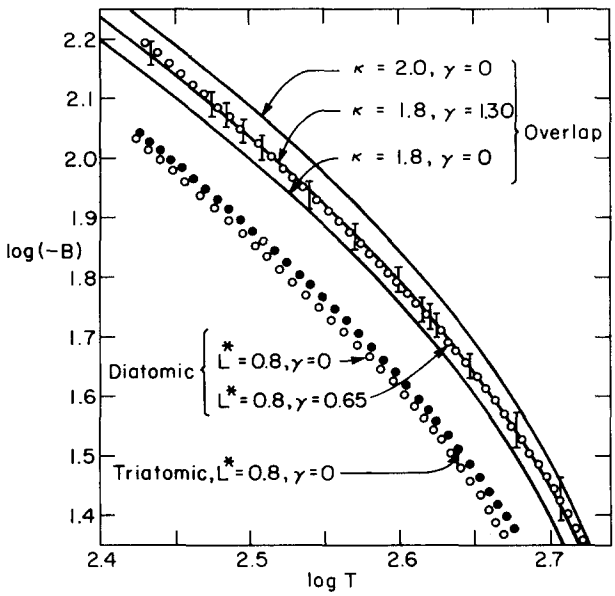

FIG. 11. Smoothed second virial coefficients of carbon dioxide are shown on a log–log plot, with an uncertainty of 2% indicated by the vertical bars. The circles show theoretical virial coefficients for the atomic models, calculated using the same values of ϵ/k, σ and L^*, but with different reduced quadrupole moments γ, or different number of atoms per molecule. The solid curves are for the overlap models with fixed ϵ/k, σ but varying shape factor κ and quadrupole moment γ.

at least in qualitative agreement with experiment.[10,11,34] (Because the diatomic and overlap potentials for N_2 are in substantial agreement, features of the two contour plots would be essentially the same. For this reason a separate contour plot for the overlap model is not given.)

IV. CARBON DIOXIDE

The difficulties encountered in successfully fitting theory to experiment were noticeably greater for the CO_2 data than for N_2. In the first place, the quadrupolar term is considerably larger for these molecules than for N_2; secondly, the overlap model does not fit both the second virial and the solid state data if a (12, 6) distance dependence is assumed.

The presence of a large quadrupole term causes the calculation of an appropriate curve of B^* versus T^*, the reduced second virial coefficient versus reduced temperature, to be time consuming and expensive. In these computations, the quadrupolar energy appears in reduced units, with a constant of proportionality $\gamma = Q^2/\epsilon\sigma^5$. One thus guesses γ; calculates B^* versus T^*; fits to experiment to determine ϵ, σ; calculates a new γ; and iterates until internal consistency is obtained.

A log–log plot of the second virial coefficients for CO_2 versus temperature[28] is shown in Fig. 11, with error bars indicating an uncertainty of ± 2 cm^3/mole in each point. Also shown are a number of theoretical curves plotted in part to show the quality of the fit between theory and experiment, and in part to show the effect of changing the parameters of the potentials. In particular, the three "atomic" curves were calculated using $\epsilon/k = 537°$; $\sigma = 3.05$ Å; this gives a good fit for a diatomic model when the reduced quadrupole constant $\gamma = 0.65$ (but this corresponds to $Q = 8 \cdot 10^{-26}$ e. s. u. cm^2, which is not equal to the experimental value for CO_2 listed in Table I). When the quadrupolar term is omitted, the calculated virial coefficients shift appreciably, as shown in Fig. 11. Since it appeared that this molecule is sufficiently long to perhaps invalidate a diatomic representation, a triatomic model was investigated (all atoms identical). Figure 11 indicates that very little change occurred when this refinement was attempted. Parameters for the final best fit of the diatomic (12, 6) potential with a quadrupole moment of 3.9×10^{-26} e. s. u. cm^2 are listed in Table III.

All the models listed in Table III give virial coefficients that fit the data with experimental error, except the one used by Suzuki and Schnepp, which was fitted to solid state data only.

Although the inclusion of such a large quadrupolar term gives rise to a noticeable shift in the parameters of the diatomic potential, the overlap model does not seem to be as sensitive to this interaction; the curves in Fig. 11 show this, as well as the fitted values of ϵ/k and σ listed in Table III. Solid CO_2 forms the same crystal lattice as α-N_2, and the calculations give a quadrupolar stabilization energy of ~1 kcal/mole in this system, which is roughly 15% of the total. Thus, for example, calculation of Suzuki and Schnepp would be in error by this amount when this energy is included. (In addition, their computed crystal lattice size will shrink by roughly 0.1 Å.)

It is interesting to note that the best overlap (12, 6) potential ($\gamma = 1.3$, $\epsilon/k = 180°$, $\sigma = 3.48$ Å, $Q = 4.1 \cdot 10^{-26}$ e. s. u. cm^2) does not give satisfactory values for the solid state properties; the theoretical stabilization energy is too small and the lattice size, too large. In contrast, the solid data are reproduced nicely by the best diatomic (12, 6) model ($\gamma = 0.90$, $\epsilon/k = 519°$, $\sigma = 2.98$ Å), and it appears that this model (or its tri-

TABLE III. Calculated properties for CO_2.

Model	ϵ/k (deg.)	σ (Å)	ΔH_{sub} (kcal/mole)	a_0 (Å)
Diatomic (12,6), $L^* = 0.8$,				
$\gamma = 0$	566	3.22	4.59	4.33
$\gamma = 0.65$	537	3.05	6.14	4.02
$\gamma = 0.90$	519	2.98	6.62	3.90
Diatomic (Suzuki and Schnepp[a]) (12,6), $L^* = 0.78$, $\gamma = 0$	770	2.95	6.48	3.94
Kihara core (12,6), $L^* = 0.69$, $\gamma = 0$	309	3.36	4.72	4.19
			5.90	4.16[b]
Triatomic (12,6), $L^* = 0.8$, $\gamma = 0$	550	3.25	4.15	4.37
Overlap (12,6), $\kappa = 1.8$,				
$\gamma = 0$	182	3.52	3.01	4.85
$\gamma = 1.3$	180	3.48	4.06	4.69
Overlap (12,6), $\kappa = 2.0$,				
$\gamma = 0$	181	3.31	3.04	4.69
Overlap (28,7), $\kappa = 1.8$,				
$\gamma = 0$	695	2.44	9.62	3.27

[a]Reference 12.
[b]Quadrupole energy added without refitting virial coefficients.

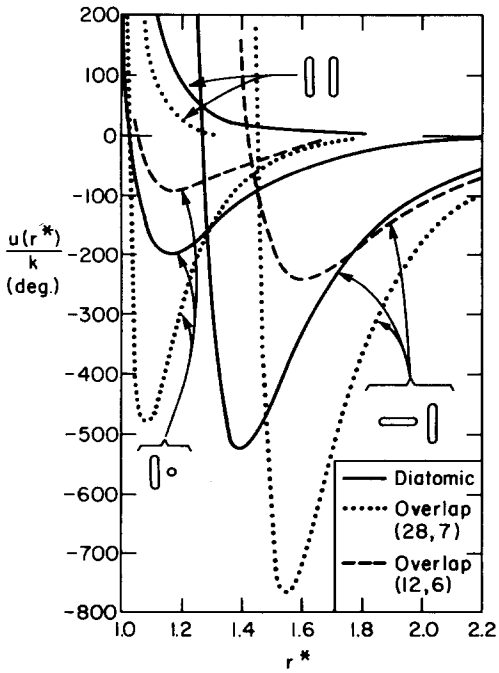

FIG. 12. The potential energy, as given by three models of the carbon dioxide interaction, is shown here as a function of distance for three fixed intermolecular orientations. (These configurations are the same as in Figs. 8 and 9.)

atomic modification) is a satisfactory representation of the interactions between CO_2 molecules. Studies of the spectrum of the van der Waals dimer (CO_2)[18] indicate that the equilibrium orientation angles are 0°, 90°, 0° (T shape) and the equilibrium distance is 4.1 Å. Curves of the interaction energy versus distance at several fixed orientations are shown in Fig. 12 for some of the potential models considered for CO_2. The minima in the curves for the best diatomic model clearly are in excellent agreement with the experimental orientation and separation ($r^* = 1.38$ or $r_{eq} = 4.11$ Å); the dissociation energy of the dimer is predicted to be 1.04 kcal/mole (experimental value unknown at present). Figure 13 shows contour plots of energy versus the polar angles Θ_1, Θ_2 for a dimer at the equilibrium separation ($r^* = 1.4$), for the planar configuration ($\phi = 0°$) and for a twisted arrangement ($\phi = 30°$). It is evident that the diatomic model energy is not very sensitive to the value of ϕ. On the other hand, the changes in energy with Θ_1, Θ_2 are much larger for $(CO_2)_2$ than $(N_2)_2$, as expected; one anticipates that at least some of the librational frequencies in the dimer will be large, in qualitative agreement with the spectral data.[18]

The fact that only one crystal structure is known for solid CO_2 can be also rationalized by the curves shown in Fig. 12, which indicate that large decreases in well depth occur as the orientations shift away from the T-shaped arrangment. Indeed, the parallel configuration of $(CO_2)_2$ is repulsive at all distances because the quadrupole repulsion overwhelms the attractive diatomic energy. This is in sharp contrast to the relatively small change in energy with angle for nitrogen that is shown in Figs. 8 and 9.

In view of the failure of the overlap (12, 6) model to reproduce the solid state properties of CO_2, other distance-dependent functions were considered. Of course, very large numbers of such functions exist which have some claim to physical reality, and one would like to have a rationale for selection that did not depend entirely upon the quality of the fit between experiment and theory. Some time ago, it was shown[35] that the potential functions for large molecules with interacting elements on their periphery tend to vary more rapidly with center-to-center distance than a (12, 6) power law. In effect, the important separations are the periphery-to-periphery distances; if the energy depends primarily on these quantities, it can change by a very large amount for a relatively small change in center-to-center separation. Indeed, it was shown that the (12, 6) law for interacting elements on the surfaces of spheres tended to give a function approximating a (28, 7) dependence on the center-to-center distance. In view of the relatively large separation of the oxygen atoms from the center of symmetry of a CO_2 molecule, it seemed reasonable to see if an overlap (28, 7) interaction would be an improvement over the (12, 6) with the same shape factor κ. A preliminary calculation where quadrupolar energies were omitted gave quite different results from the (12, 6), $\gamma = 0$ function, as is shown in Table III. The parameters that fitted the virial coefficients give solid state energies that are larger and lattice parameters that are smaller than the experimental values. It appears that the overlap model with a distance function having indices intermediate between (12, 6) and (28, 7) would give a satisfactory representation of the CO_2 interaction. At this stage, the choice of power law seemed too arbitrary to warrant further computation; hopefully, future studies will give some kind of independent criterion for this choice.

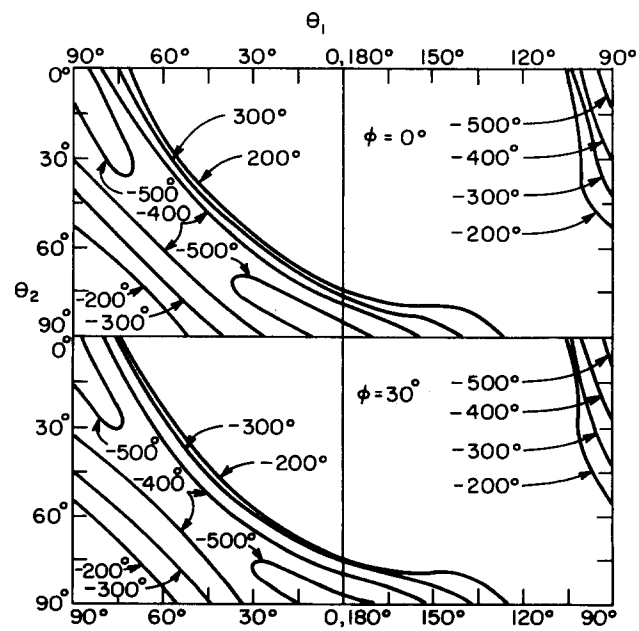

FIG. 13. Equipotential contours for the diatomic model (plus quadrupole energy) of interacting carbon dioxide molecules are shown here for varying polar angles, but with r^* fixed at 1.4 and with ϕ fixed first at 0° and then at 30°.

TABLE IV. Calculated properties for benzene.

	ϵ/k (deg.)	σ (Å)	ΔH_{sub} (kcal/mole)	a_0 (Å)
Kihara core (see text), $\gamma = 0$	740	3.6	10.2	7.6
Overlap (12,6), $\kappa = 0.5$, $\gamma = 0.005$	176	12.1	2.4	15.1
$\gamma = 0.007$	195	11.2	2.7	14.2
Overlap (28,7), $\kappa = 0.5$, $\gamma = 0.0$	912	5.76	8.8	7.23
$\gamma = 0.039$	912	5.76	9.9	7.21

The dotted and dashed lines in Fig. 12 show the overlap (28, 7) and (12, 6) energies calculated for several fixed orientations using the parameters listed in Table III [but including quadrupolar terms for the (28, 7)]. The curves exhibit the same general characteristics as the diatomic model, which tends to give energies intermediate between the overlap (28, 7) and (12, 6) calculations; presumably, an intermediate power law in the overlap model would give energies that would lie reasonably close to the curves for the best diatomic model.

V. BENZENE

The benzene molecule is an excellent example of a simple nonlinear molecule. The crystal structure of benzene (at low pressure) is orthorhombic, with cell dimensions 7.29, 9.47, and 6.74 Å at 78 °K.[36] The solid state[36,37] and second virial coefficient data have previously been fitted[3] to the Kihara model using a hexagonal core of edge length 1.94 Å. The shape of the molecule defined by this model is thus hexagonal, with thickness 3.6 Å and corner-to-corner size 7.5 Å. The parameters of this model that fit the virial coefficients are listed in Table IV. Using a simplified expression for the known molecular orientations, the Kihara potential gives rise to a minimum in the energy at unit cell dimensions of 7.6, 11.0, and 6.9 Å; as can be seen in Tables I and IV, the theoretical and experimental ΔH_{sub} are also in good agreement. However, this calculation suffers from omission of the quadrupolar energy.

A major problem encountered in studies of the benzene system is caused by uncertainties in the second virial coefficient data[28,38] which have been measured over a relatively narrow range of temperature. The result is a rather severe problem in determining the "best fit" ϵ and σ for a given model. This is illustrated in Fig. 14, where a 5% uncertainty in the smoothed experimental points[28] is indicated by the vertical lines; some recent experimental data[38] (with a stated precision of ~1%) are shown by the points. In fact, the range of ϵ and σ that give a fit of the overlap model to these data is so large that other criteria were introduced in an attempt to optimize the values. Specifically, σ was chosen so that the size of the benzene molecule conformed to preconceived notions; i.e., so that the correct lattice size was obtained, if possible.

The overlap model with a (12, 6) potential plus quadrupolar interactions was first fitted to the data using the semiempirical estimate[39] of Q listed in Table I. The "best fit" curve is shown in Fig. 14; a κ value of 0.5 was chosen for the oblate ellipsoid that represents the molecular shape, giving a molecule with thickness equal to half its diameter. Since the σ value listed in Fig. 14 (and in Table IV) for the (12, 6) model corresponds to the diameter, the thickness would be 6 Å. These dimensions are unreasonably large for a benzene molecule. (Similarly large dimensions have been obtained from the virial coefficients for a model composed of a spherical Lennard-Jones (12, 6) function plus quadrupolar terms.[40]) Figure 14 also shows the theoretical curve for the smallest σ that still gives a fit to the data (within 5% uncertainty); this value of σ is still much too large to be realistic. Consequently, the overlap (28, 7) model plus quadrupolar terms was studied; although the best fit curve still corresponded to an excessively large σ, a theoretical curve could be constructed that fits the data reasonably well with a σ value that also is capable of accounting for the solid properties. This is shown by the solid curve in Fig. 14, and the calculated solid state properties are listed in Table IV. It is evident that this model can be forced into agreement with both the virial coefficient and the solid state data.

If we now take this overlap (28, 7) as the best available representation of the benzene–benzene interaction, curves of energy versus distance at fixed orientation can be constructed, as shown in Fig. 15. We see that the T-shaped dimer is the most stable (after the quad-

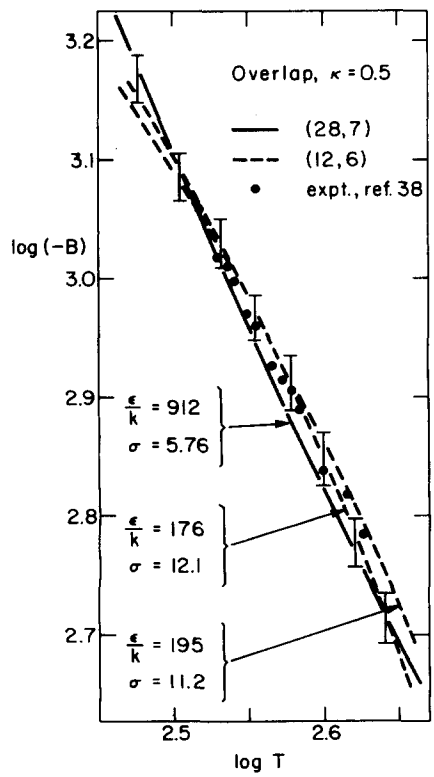

FIG. 14. The smoothed values of the experimental second virial coefficients of benzene, with an uncertainty of 5%, are indicated by the vertical lines; a recent set of measurements is shown by the points, and the curves show the fit between experiment and the theoretical virial coefficients calculated for the overlap model (plus quadrupole energy) with fixed shape but for different choices of potential parameters and for different power laws for the distance dependence of the interaction.

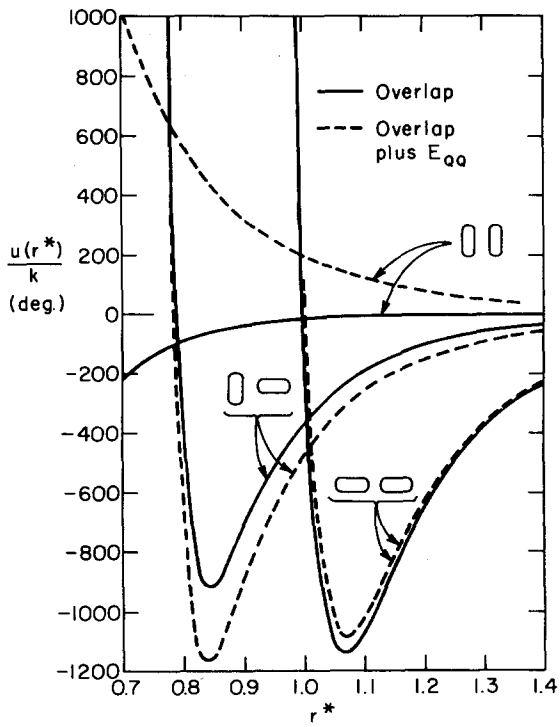

FIG. 15. The interaction energy of a pair of benzene molecules with fixed orientation is plotted as a function of separation distance. The potential is calculated from the overlap model and a (28,7) power law, with and without quadrupolar energy E_{QQ}. The orientations chosen are the following: face-to-face (θ_1, θ_2, $\phi = 0°$, 0°, anything); end-to-end (90°, 90°, 0°); and T-shaped (0°, 90°, anything).

rupolar energy is included), and one predicts that a van der Waals molecule $(C_6H_6)_2$ should form with this configuration, an intermolecular separation of 4.8 Å and a dissociation energy of 2.3 kcal/mole. The fact that the minimum energy in the end-to-end configuration is quite close to that for the T-shape indicates that more than one solid phase of benzene may exist, in agreement with the experimental finding of a high pressure monoclinic solid in addition to the orthorhombic phase. It is interesting to note that an x-ray study indicates that an important difference between the two phases is that "the ring planes are more nearly parallel in the monoclinic phase."[15]

The quadrupole repulsion causes the face-to-face orientation to be repulsive at all distances, as shown in Fig. 15; without the electrostatic energy, the overlap model would predict a minimum energy of −2.3 kcal/mole at $r^* = 0.53$ for a pair of benzene molecules in this orientation.

In other studies,[8,14,15] one of the most popular potential energy models for benzene has been an atomic model (which unfortunately does not include quadrupolar energies). In this case, the very large number of terms (144) in the summation of Eq. (1.2) prohibits the use of this model for any but the most restricted problems; nevertheless, calculations of the lattice modes of both crystalline modifications have been performed[14] in which the molecular positions in the crystals were taken as known quantities. Even though the calculated frequencies agree well with the spectral data for solid benzene, it is difficult to see how one could utilize this model in studies of either the liquid or the gas.

VI. DISCUSSION

The intermolecular potential functions obtained in this work can obviously be used in a variety of ways. In addition to the calculations of solid state lattice structure and intermolecular frequencies, and the properties of the van der Waals dimers alluded to previously, studies of equilibrium and dynamics of the liquid can be performed either by computer simulation[41] or by using one of the more successful theories of the liquid state.[1,22,23] For examples, molecular dynamics computations of the orientational time-correlation functions for benzene have been performed using the overlap (12, 6) potential without quadrupolar terms.[42] It would be of interest to compare these results with calculations that utilize the overlap (28, 7) potential, and which include the quadrupolar interaction. Inasmuch as Fig. 15 indicates that the presence of electrostatic terms strongly affects the probability of face-to-face orientations of pairs of benzene molecules in the fluid, one might anticipate that such terms will have a large effect on the angular correlations, static or dynamic.

Of course, it is straightforward to compute angular correlations for the dilute gas. For example, in the limit of zero density, one has

$$\langle \cos^2\Theta_{ij} \rangle = \frac{\int\cdots\int \cos^2\Theta_{ij} \exp[-u(r, \Omega_1, \Omega_2)/kT]\, d\Omega_1 d\Omega_2}{\int\cdots\int \exp[-u(r, \Omega_1, \Omega_2)/kT]\, d\Omega_1 d\Omega_2}, \tag{6.1}$$

where $\cos\Theta_{ij} = \cos\Theta_i \cos\Theta_j + \sin\Theta_i \sin\Theta_j \cos\phi$. At large separation distances, $\langle \cos^2\Theta_{ij} \rangle$ approaches the random

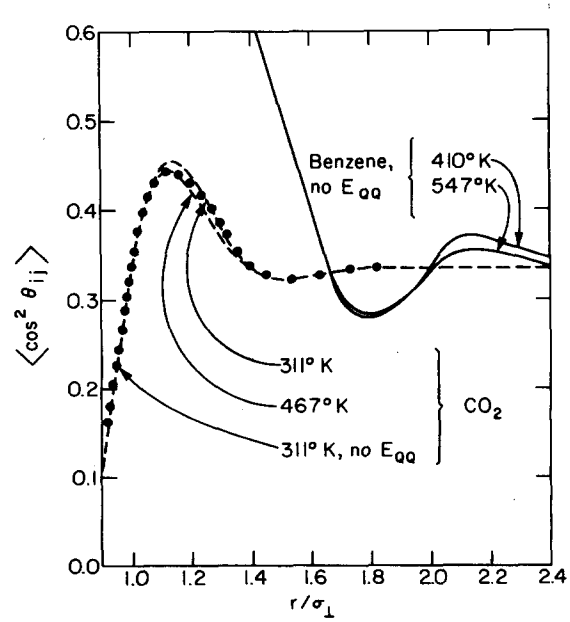

FIG. 16. The mean square cosine of θ_{ij}, the angle between molecular symmetry axes, is plotted as a function of reduced distance for CO_2 and benzene. In each case, the average was performed at two temperatures in the limit of zero density. The effect of omitting quadrupolar energy upon angular correlation for CO_2 at 311 °K is shown by the points.

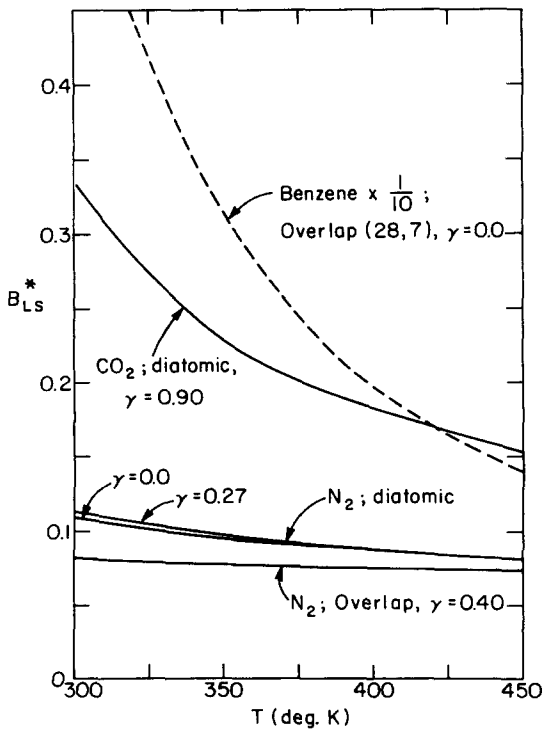

FIG. 17. Computed values of the depolarized light scattering virial coefficient are shown as a function of temperature for best fit models. Curves for N_2 were obtained for the diatomic model; with and without quadrupolar energy and for the overlap (12,6) model, with quadrupole energy; for CO_2, the diatomic model with the overlap (28, 7) model without quadrupole terms was used. The values calculated for benzene are quite large and thus are reduced by a factor of ten in order to fit them on the figure.

orientation value of 1/3; at smaller r, this quantity will deviate from its limiting value as angular correlations become important. Figure 16 shows curves of $\langle \cos^2\Theta_{ij} \rangle$ calculated using the diatomic (12, 6) model for CO_2 with and without quadrupolar energy and the overlap (28, 7) model without quadrupolar energy for benzene. It is evident that a sharp rise in $\langle \cos^2\Theta_{ij} \rangle$ occurs as r^* approaches unity for this representation of benzene; this corresponds to the large preference for face-to-face orientations (with $\Theta_{ij} = 0°$) at these diatances. Of course, the probability of finding a pair of benzene molecules at r^* less than 0.8 is quite small unless one omits E_{QQ}, as indicated by the curves in Fig. 15. Since this corresponds to r/σ less than 1.6, the behavior of $\langle \cos^2\Theta_{ij} \rangle$ at these distances is of no importance, physically.

It should be emphasized that a value of $\langle \cos^2\Theta_{ij} \rangle \simeq \frac{1}{3}$ does not necessarily mean that all orientations are energetically equivalent; for example, the curves for CO_2 in Fig. 16 pass through this point at $r^* = 1.4$; however, the energy contours in Fig. 13 were computed for this separation and show a strong dependence upon angle. If we recollect that $\cos^2\Theta = \frac{1}{3}$ for the "magic angle" $\Theta = 55°$, we see that an apparently random value can also result from a probability distribution that is symmetric about $\Theta_{ij} = 55°$.

An observable that is explicitly dependent upon static orientational correlations is the intensity of depolarized light scattering.[43] If one expands this quantity as a power series in the density, a depolarized light scattering second virial coefficient B_{LS} that accounts for all but the collision-induced scattering can be defined as

$$B^*_{LS} = \frac{B_{LS}}{4\pi\sigma^3} = \int\int (\tfrac{3}{2}\cos^2\Theta_{ij} - \tfrac{1}{2}) \times \exp\left[\frac{-u(r, \Omega_1, \Omega_2)}{kT}\right] r^{*2} dr^* \frac{d\Omega}{4\pi} 1 \frac{d\Omega}{4\pi} 2 \ . \quad (6.2)$$

Figure 17 shows curves of B^*_{LS} calculated for the best models of each gas considered. It is interesting to note that the values for the planar benzene molecule are considerably larger than those for the linear CO_2; it is not surprising to find small B^*_{LS} for the weakly nonspherical N_2, especially at the relatively high temperatures shown in the figure. It is unfortunate that experimental data of this kind are apparently unavailable at present, since they are one of the most direct measures of orientational correlation known.

Although the research reported in this paper was initially aimed at comparing the overlap model with some other, better known representations of nonspherical molecules, several additional results were obtained in the process. Hopefully, the best-fit potential functions obtained for the three nonspherical molecules considered here will prove useful in future statistical mechanical studies of these substances; more detailed experimental characterizations of the properties of the van der Waals dimers of these and other simple systems should be extremely helpful in determining the intermolecular interaction laws; and a reconsideration of calculations of solid state properties (such as spectral frequencies) is suggested in which potential functions are employed that are simple enough to be useful in studies of the liquid and the gas, but realistic enough to give theoretical crystal structures and lattice frequencies that agree with experiment.

We note that our experience with the overlap model indicates that the most appropriate values of the indices (m, n) in a power law expression for the distance dependence of the energy appear to increase as the molecular shape becomes more nonspherical; it seems likely that this is a consequence of the presence of interacting elements (atoms or regions of high electron density) at large distances from the molecular center of symmetry. The development of criteria for choosing (m, n) for a given molecular structure would be an important step in developing the overlap model into a convenient, realistic representation of the nonelectrostatic part of the intermolecular interaction energy of polyatomic molecules.

*This work supported by grants from the National Science Foundation.

†Present address: Union Carbide Corp., Technical Center, South Charleston, West Virginia 25314

[1]However, see M. S. Anath, K. E. Gubbins, and C. G. Gray, Mol. Phys. **28**, 1005 (1974); K. E. Gubbins, C. G. Gray, P. A. Egelstaff, and M. S. Anath, Mol. Phys. **25**, 1353 (1973).

[2]T. Kihara, Rev. Mod. Phys. **25**, 831 (1953); Adv. Chem. Phys. **5**, 147 (1963).
[3]T. Kihara and S. Koba, J. Phys. Soc. Jpn. **14**, 247 (1959); S. Koba, J. Phys. Soc. Jpn. **16**, 627 (9161).
[4]A. Koide and T. Kihara, Chem. Phys. **5**, 34 (1974).
[5]A. Mueller, Proc. R. Soc. A **154**, 624 (1936).
[6]D. E. Williams, J. Chem. Phys. **45**, 3770 (1966); **47**, 4680 (1967).
[7]A. I. Kitaigorodsky, *Molecular Crystals and Molecules* (Academic, New York, 1973), H. A. Scheraga, Adv. Phys. Org. Chem. **6**, 1031 (1968).
[8]F. A. Momany, G. Vanderkooi, and H. A. Scheraga, Proc. Natl. Acad. Sci. **61**, 429 (1968).
[9]N. Jacobi and O. Schnepp, J. Chem. Phys. **58**, 3647 (1973).
[10]T. S. Kuan, A. Warshel and O. Schnepp, J. Chem. Phys. **52**, 3012 (1970); O. Schnepp and A. Ron, Discuss. Faraday Soc. **48**, 26 (1969); B. C. Kohin, J. Chem. Phys. **33**, 882 (1960).
[11]J. C. Raich and R. L. Mills, J. Chem. Phys. **55**, 1811 (1971); J. C. Raich, N. S. Gillis and A. B. Anderson, *ibid.* **61**, 1399 (1974); P. V. Dunmore, *ibid.* **57**, 3348 (1972); J. Felsteiner and Z. Friedman, Phys. Rev. B **8**, 3996 (1973).
[12]M. Suzuki and O. Schnepp, J. Chem. Phys. **55**, 5349 (1971); T. G. Gibbons and M. L. Klein, *ibid.* **60**, 112 (1974).
[13]D. A. Dows and L. Hsu, J. Chem. Phys. **56**, 6228 (1972); J. R. Sweet and W. A. Steele, *ibid.* **47**, 3022, 3029 (1967); **50**, 668 (1969).
[14]G. Taddei, H. Bonadeo, M. P. Marzocchi, and S. Califano, J. Chem. Phys. **58**, 966 (1973); D. A. Oliver and S. H. Walmsley, Mol. Phys. **17**, 617 (1969); W. D. Ellenson and M. Nicol, J. Chem. Phys. **61**, 1380 (1974).
[15]G. J. Piermarini, A. D. Mighell, C. E. Weir, and S. Block, Science **165**, 1250 (1969).
[16]C. A. Long and G. E. Ewing, J. Chem. Phys. **58**, 4824 (1973); S. E. Novick, P. B. Davies, T. R. Dyke and W. Klemperer, J. Am. Chem. Soc. **95**, 8547 (1973).
[17]G. E. Ewing, Angew, Chem. (Intern. Ed.-English) **11**, 486 (1972).
[18]L. Mannick, J. C. Stryland, and H. L. Welsh, Can. J. Phys. **49**, 3056 (1971).
[19]R. J. LeRoy and J. Van Kranendonk, J. Chem. Phys. **61**, 4750 (1974).
[20]H. Goldstein, *Classical Mechanics* (Addison–Wesley, Cambridge, MA, 1950), Sec. 4.4.
[21]B. J. Berne and P. Pechukas, J. Chem. Phys. **56**, 4213 (1972).
[22]W. A. Steele and S. I. Sandler, J. Chem. Phys. (to be published); A. Das Gupta, S. I. Sandler, and W. A. Steele, J. Chem. Phys. **62**, 1769 (1975). S. I. Sandler, Mole. Phys. **28**, 1207 (1974).
[23]S. Sung and D. Chandler, J. Chem. Phys. **56**, 4989 (1972); L. J. Lowden and D. Chandler, *ibid.* **61**, 5228 (1974).
[24]J. A. Barker and D. Henderson, Annu. Rev. Phys. Chem. **23**, 439 (1972); W. R. Smith, Spec. Per. Report (Statistical Mechanics) **1**, 71 (1973).
[25]W. A. Steele, J. Chem. Phys. **39**, 3197 (1963).
[26]A. D. Buckingham, Adv. Chem. Phys. **12**, 107 (1967).
[27]L. Pauling, *Nature of the Chemical Bond* (Cornell University, Ithaca, 1948).
[28]J. H. Dymond and E. B. Smith, *Tables of Virial Coefficients of Gases. A Critical Compilation* (Clarendon, Oxford, 1969).
[29]K. K. Kelley, Bull, U. S. Bur. Mines **383** (1935).
[30]T. H. Jordan, H. W. Smith, W. E. Streib, and W. N. Lipscomb, J. Chem. Phys. **41**, 756 (1964); A. F. Schuch and R. L. Mills, *ibid.* **52**, 6000 (1970).
[31]D. E. Stogryn and A. P. Stogryn, Mole. Phys. **11**, 371 (1966).
[32]J. A. Pople, Proc. R. Soc. A **221**, 508 (1954).
[33]J. de Smedt and W. H. Keesom, Prod. Acad. Sci. Amsterdam **27**, 930 (1924); Z. Krist. **62**, 312 (1926); H. Mark and E. Pohland, Z. Krist. **61**, 293 (1925); **64**, 113 (1926); J. C. McLennon and J. O. Wilhelm, Trans. R. Soc. (Canada) III **19**, 51 (1925).
[34]F. D. Medina and W. B. Daniels, J. Chem. Phys. **59**, 6175 (1973).
[35]H. G. David, S. D. Hamann, and R. B. Thomas, Aust. J. Chem. **12**, 309 (1959); A. G. de Rocco, T. H. Spurling and T. S. Storvick, J. Chem. Phys. **46**, 599 (1967); A. G. de Rocco and W. G. Hoover, *ibid.* **36**, 916 (1962); S. D. Hamann and J. A. Lambert, Aust. J. Chem. **7**, 1 (1954).
[36]E. G. Cox, D. W. J. Cruikshank and J. A. S. Smith, Proc. R. Soc. A **247**, 1 (1958); G. E. Bacon, N. A. Curry, and S. A. Wilson, *ibid.* **279**, 98 (1964).
[37]A. Bondi, J. Chem. Eng. Data **8**, 371 (1963); N. Wakayama and M. Inokuchi, Bull. Chem. Soc. Jpn. **40**, 2267 (1967).
[38]P. G. Francis, M. L. McGlashan, and C. J. Wormald, J. Chem. Thermodyn. **1**, 441 (1969).
[39]R. L. Shoemaker and W. H. Flygare, J. Chem. Phys. **51**, 2988 (1969).
[40]G. A. Bottomley and T. H. Spurling, Aust. J. Chem. **19**, 1331 (1966).
[41]J. Barojas, D. Levesque, and B. Quentrec, Phys. Rev. A **7**, 1092 (1973); S. S. Wang, C. G. Gray, P. A. Egelstaff, and K. E. Gubbins, Chem. Phys. Lett. **21**, 123 (1973); S. S. Wang, P. A. Egelstaff, C. G. Gray, and K. E. Gubbins, *ibid.* **24**, 453 (1974); G. N. Patey and J. P. Valleau, J. Chem. Phys. **61**, 534 (1974).
[42]J. N. Kushick, Ph.D. thesis, Columbia University, 1974.
[43]H. Benoit and W. Stockmayer, J. Phys. Radium **17**, 21 (1956); S. Kielich, J. Chem. Phys. **46**, 4090 (1967).